ISSN: 1411-3082

NUMERICAL SIMULATION OF FLOW OVER TWO-DIMENSIONAL MOUNTAIN RIDGE USING SIMPLE ISENTROPIC MODEL

Siswanto [1, 2]
[1] *Graduate School of Climate Sciences, University of Bern*
[2] *National Agency for Meteorology, Climatology and Geophysics, Republic of Indonesia*

ABSTRACT

The aim of this work is to study turbulent flow over two-dimensional hill using a simple isentropic model. The isentropic model is represented by applying the potential temperature θ, as the vertical coordinate and is conversed in adiabatic flow regimes. This implies a vanishing vertical wind in isentropic coordinates which reduces the three dimensional system to a stack of two dimensional θ – layers. The equations for each isentropic layer are formally identical with the shallow water equation. A computational scheme of centered finite differences is used to formulate an advective model. This work reviews a simple isentropic model application to investigate gravity wave and mountain wave phenomena regard to different experimental design of computation and topographic height.

Keywords: atmospheric flow, gravity wave, isentropic coordinates, model, two-dimensional system.

ABSTRAK

Model sederhana isentropis telah diaplikasikan untuk mengidentifikasi perilaku aliran masa udara melewati topografi sebuah gunung. Dalam model isentropis, temperature potensial θ digunakan sebagai koordinat vertikal dalam rezim aliran adiabatis. Medan angin dalam arah vertical dihilangkan dalam koordinat isentropis sehingga mereduksi sistim tiga dimensi menjadi sistim dua dimensi lapisan θ. Skema komputasi beda hingga tengah telah digunakan untuk memformulasikan model adveksi. Paper ini membahas aplikasi sederhana dari model isentropis untuk mempelajari gelombang gravitas dan fenomena angin gunung dengan desain komputasi periodic dan kondisi batas lateral serta simulasi dengan topografi yang berbeda.

Kata Kunci: aliran atmosfer, gelombang gravtasi, koordinat isentropis, model dua dimensi.

1. INTRODUCTION

The earth's troposphere is the portion of the atmosphere where radiation and dominant mechanisms of vertical heat transfer such as convection takes place. At the mid-latitudes this occurs up to a height of about 10km while in the low latitudes the troposphere has a higher altitude. Although it is composed of gases, in many ways the atmosphere behaves like a fluid, and hence, many atmospheric disturbances occur as waves. These atmospheric disturbances result from the interactions of several forces including pressure gradient, Coriolis force, gravity, and friction

Since the friction effect of surface's terrain shape such as a mountain profile is very important and has to be considered for the local to mesoscale atmospheric dynamic, for example, it has important aspect for the study of gravity wave mechanisms which may include geostrophic adjustment, shear instability, convection, and topography, hence, modeling of flow over the mountain is then more relevant to understanding of the physics of stratified atmosphere studies, particularly to study mountain wave and downslope winds in relation to aircraft incident around the mountain area. As long as the atmospheric conditions include a stable atmosphere with strong winds oriented perpendicular to the mountain range, mountain waves and downslope wind are likely. This is true regardless of the location and orientation of the mountains. In Indonesia, some mountain waves are well known such as Angin Koembang in Java and Wambraw in Papua which probably responsible to the aircraft incident around these area.

For these purposes, the inviscid Euler equations are taken as the starting point for the model.

$$\frac{Du}{Dt} = -\frac{1}{\rho}\nabla p - gk, \qquad (1.1)$$

$$\frac{\partial \rho}{\partial t} + \nabla.(\rho u) = 0 \qquad (1.2)$$

where u is the velocity vector, ρ is density, p is pressure and k is the unit vector in the z direction, g is the gravitational constant, and the 2D advection derivative is defined as

$$\frac{D}{Dt} = \frac{\partial}{\partial t} + u\frac{\partial}{\partial x} + w\frac{\partial}{\partial z}$$

Typically in the atmospheric modeling a number of simplifying assumption are made. Firstly, the Boussineq approximation is assumed that the effect of density fluctuations on the conservation of mass (continuity equation) and inertia can be ignored, but that buoyancy forces must be accounted for. For the hydrostatic approximation, p and ρ are then splitted into a vertical profile -hence stratification - and small disturbances to that profile

$$\rho(x,z,t) = \rho^0 + \bar{\rho}(x,z,t)$$

$$p(x,z,t) = p^0 + \bar{p}(x,z,t)$$

these approximations have been discussed in detail in Durran (1998). Now from (1.1) and (1.2) can be written as :

$$\rho^0\frac{Du}{Dt} = -\nabla p - \rho g k \qquad (1.3)$$

$$\nabla.u = 0 \qquad (1.4)$$

If we assume the troposphere behaves ideally, then we can have a look to the thermodynamic properties of an ideal gas. The equation of state for an ideal gas is

$$p = \frac{R}{M}\rho T \qquad (1.5)$$

where M is the molecular weight, T is the temperature, and R is the universal gas constant. The first law of thermodynamics states that for a unit mass

$$dq = c_v\, dT + p\, dV \qquad (1.6)$$

where q is the heat transferred into the system, c_v is the heat capacity at constant volume, and V is the volume. Differentiating (1.5) and considering that $\rho = 1/V$, leads to

$$p\, dV + V dp = \frac{R}{M} dT \qquad (1.7)$$

Substituting (1.7) into (1.6) and using the fact that for an ideal gas $R/M = c_p - c_v$ where c_p is the heat capacity at constant pressure, therefore, the thermodynamic equation can be expressed as

$$dq = c_p\, dT - V\, dp \qquad (1.8)$$

From these equation, we can derive the expression of entropy in an ideal gas,

$$S = c_p\, lnT - (c_p - c_v) ln\, p + C \qquad (1.9)$$

An adiabatic process is one in which there is no heat transfer across the system boundary (entropy remains constant). From (1.9) we can realize that if air is brought to some reference pressure adiabatically, its temperature at that point, which is defined as the potential temperature θ, can be expressed as

$$\theta = T\left(\frac{p_{ref}}{p}\right)^{\kappa} \text{ or } \theta = T\left(\frac{p_{ref}}{p}\right)^{R/c_p} \quad (1.10)$$

In the isentropic system, potential temperature serves as the vertical coordinate. Here p_{ref} = 1000 hPa denotes a reference pressure, R = 287 J/K.kg is the gas constant for dry air, and c_p=1004 J/K.kg the specific heat of dry air at constant pressure.

The vertical wind in isentropic coordinates is then defined as (Schär C. , 2008)

$$\dot{\theta} := \frac{D\theta}{Dt} \quad (1.11)$$

and is measured in [Ks^{-1}]. For adiabatic flows $\dot{\theta} = D\theta/Dt = 0$ for instance the vertical wind vanishes and the flow becomes quasi-horizontal on the θ-surfaces. This is an important simplification in numerical implementation especially for idealized studies of adiabatic flows in isentropic coordinates. However, the invertibility condition of coordinate transformations requires that $\theta = \theta(z)$ and $\theta = \theta(p)$ are strictly monotonic functions, i. e.

$$\frac{\partial\theta}{\partial z} > 0 \text{ and } \frac{\partial\theta}{\partial p} < 0 \quad (1.12)$$

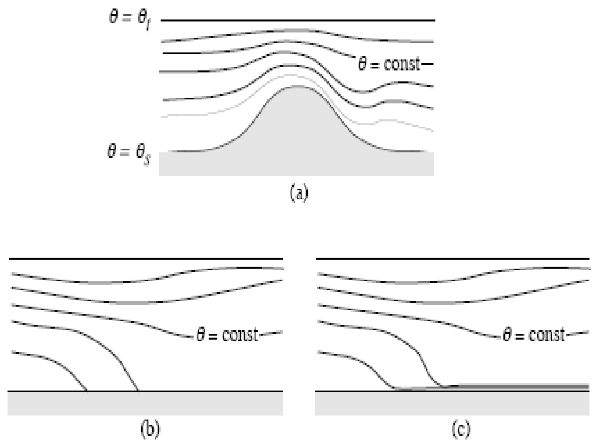

Figure 1. Vertical section of isentropic coordinates in (a) an idealized stratified flow over a mountain, and (b,c) in a frontal zone. Panel (c) show how the lower boundary condition may be represented by theta-layers of vanishing thickness (see Schär, 2009)

In this adiabatic case some simplifying assumptions are also applied such as : neglect earth's rotation (f = 0), adiabatic flow is considered as $\dot{\theta} = D\theta/Dt = 0$, two-dimensional flow in (x,z) plane, therefore $\frac{\partial}{\partial y} = 0$, $v = 0$, and the lower boundary is an isentropic surface $\theta_{(z=z_s)} = \theta_s = constant$.

These conditions are often not met in the lower troposphere or in the planetary boundary layer. Thus, isentropic coordinates are not suited for realistic weather prediction or climate model, or only in combination with other coordinates (e.g. $\sigma - p - \theta$-hybrid coordinate). An additional disadvantage of isentropic coordinate is due to notorious difficulties at the lower boundary. For certain idealized problems (such as adiabatic flows past mountain ridges) the lower boundary may be represented by a surface of constant potential temperature (Fig. 1.a). In general, however, atmospheric flows are baroclinic (e.g. horizontal temperature gradients in frontal zones) and the lower boundary contains some temperature contrast (Fig.1.b). In these cases, near-surface isentropic layers may be represented as collapsed massless layers (Fig.1.c), which yields a difficult numerical problem.

2. ISENTROPIC FORM OF GOVERNING EQUATIONS

In this project work, an isentropic model for an adiabatic, two-dimensional flow over a bell shape mountain ridge $ae^{-(x_i/b)^2}$ is presented. The equations for each isentropic layer are then formally identical with the shallow water equations.

Firstly, the potential temperature (1.10) is used to eliminate pressure from the equation of state. Manipulation of the horizontal momentum equation $\frac{DV}{Dt} + f(k \times V) = -\nabla p\phi$ in the pressure coordinates after transformation of the pressure force in the isobaric form $(\partial\phi/\partial x)_p$, and furthermore, by introducing

$\partial\phi/\partial p = -1/\rho$ and $1/\rho = RT/p$, briefly, these steps yielding :

$$\frac{RT}{p}\left(\frac{\partial p}{\partial x}\right)_\theta = \frac{RT}{p_{ref}}\left(\frac{\theta}{T}\right)^{c_p/R}$$

$$p_{ref}\left(\frac{\partial}{\partial x}\right)_\theta\left(\frac{T}{\theta}\right)^{c_p/R} = \left(\frac{\partial\, c_pT}{\partial x}\right)_\theta \qquad (2.1)$$

$$\frac{Du}{Dt} - fv = -\left(\frac{\partial M}{\partial x}\right)_\theta ,$$

$$\frac{Dv}{Dt} - fu = -\left(\frac{\partial M}{\partial y}\right)_\theta \qquad (2.2)$$

where $M = \phi + c_pT = gz + c_pT$ (2.3)

is describing the Montgomery potential that plays the same role as the geopotential in pressure coordinates (in some references this also similar with Montgomery streamfunction ψ, see i.e in Holton, 2004). To define the isentropic mass density (or isentropic density), it is common to use sigma coordinate $\sigma := -\frac{1}{g}\frac{\partial p}{\partial\theta}$ whereupon $\rho\, dz = \sigma\, d\theta$. The isentropic density σ plays the same role as density ρ in *z*-coordinate. Thus, the isentropic continuity equation from the *z*-coordinate is stated as

$$\frac{\partial\sigma}{\partial t} + \left(\frac{\partial\sigma u}{\partial x}\right)_\theta + \left(\frac{\partial\sigma v}{\partial y}\right)_\theta + \frac{\partial\sigma\dot\theta}{\partial\theta} = 0 \qquad (2.4)$$

and the hydrostatic relation in the isentropic model is expressed as the Exner function (Holton, 2004) :

$$\pi = \frac{\partial M}{\partial\theta} \quad \text{with} \quad \pi = c_p\left(\frac{p}{p_{ref}}\right)^{\kappa/c_p} \qquad (2.5)$$

As with the shallow water system, equation (2.2) and (2.4) can be combined and therefore resulted a conservative flux of the momentum equation in the x-direction :

$$\frac{\partial(\sigma u)}{\partial t} + \left(\frac{\partial(u\sigma u)}{\partial x}\right)_\theta + \left(\frac{\partial(v\sigma u)}{\partial y}\right)_\theta + \frac{\partial(\dot\theta\sigma u)}{\partial\theta} - f\sigma u = -\sigma\left(\frac{\partial M}{\partial y}\right)_\theta \qquad (2.6)$$

Regarding the boundary condition problems, in the isentropic model therefore we assume that the domain is confined at the surface and the model top by quasi-horizontal surfaces of constant potential temperature θ_s and θ_t, respectively. We also may assume that the top surface is horizontal (rigid lid) and characterized by constant pressure, i.e. $p_{(\theta=\theta_t)} = p_t = constant$, and at the lower boundary, the height of topography determines the geopotential, as in pressure coordinates, i.e. $\phi_{(\theta=\theta_s)} = gz_s$

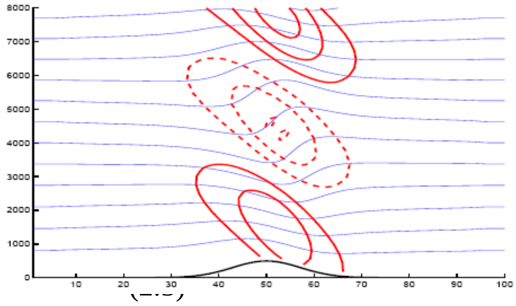

Figure 2. Gravity wave caused by adiabatic flow past a hill. Flow is from left to right. Potential temperature denotes as thin blue lines and horizontal wind as thick red lines. (see Schär, 2009, exercise part.)

3. NUMERICAL METHOD

The momentum equation in advective (2.2) or flux form (2.6), the continuity equation (2.4), the hydrostatic relation (2.5), the definition of the isentropic density σ, and the boundary condition together yield a complete prognostic set of governing equations. Here a simple numerical scheme is presented that employs ideas familiar from the treatment of the shallow water equations. In addition to the horizontal staggering, the variables are also staggered in the vertical direction as described below

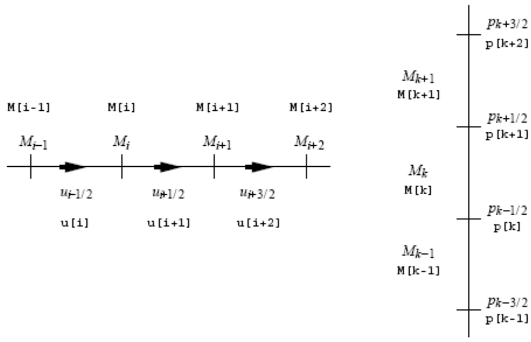

Figure 3. Staggering of the variables in horizontal and vertical dimensions. These are applicable for ui+1/2,k horizontal wind, σi,k for isentropic density, Mi,k for Montgomery potential, pi,k+1/2 for pressure, and for Exner function πi,k+1/2.

Discretization of those equations using centered finite different (Fig. 3), yield:

$$\chi_k = \chi[\theta = \theta_s + (k-1/2)\Delta\theta]$$

$$\sigma_{i,k}^{n+1} = -\frac{p_{i,k+1/2}^{n+1} - p_{i,k-1/2}^{n+1}}{g\Delta\theta}$$

$p_0(\theta_t) = p_{i,k=nz+1/2}^{n+1}$, where nz = number of vertical layers.

Montgomery potential is discretized as :

$$M_{i,k=1}^{n+1} = M_{i,k=1/2}^{n+1} + \frac{\Delta\theta}{2}\pi_{i,k=1/2}^{n+1}$$

All the discretizations have been done in the matlab code run and resulting model outputs which are presented in the following part.

Initial conditions had been set up as the model has been started with a one-dimensional profile where the layer thickness was set constant. The next step is then to calculate the topography where the mountain has been projected as bell shape function to represent terrain profiles. Evaluations of wave drag as a function of mountain height will be presented and discussed. The initial vertical stratification is given by the Brunt-Väisälä frequency. The model can then be improved by using relaxing lateral boundary conditions and absorbing boundary at the top of the isentropic profile.

4. RESULT AND DISCUSSION

As stated at the beginning, the terrain of the earth influences the atmospheric flow at all levels and on scales ranging from the sheltering effect of small rocks to planetary waves generated by the mountain ranges. The terrain can influence the atmosphere in various ways. The wind may be obstructed directly by mountains and the mountains can generate gravity waves or inertial waves that propagate in all directions far away from their source. The mountains also affect the horizontal and vertical distribution of solar heating in the troposphere and through their effect on the vertical flow field. If a particle of air is displaced vertically from its level of equilibrium it returns back in an oscillating movement around its original level. These oscillations are usually called mountain waves.

In this part, the outputs of isentropic model experiment are visualized in two dimensional space (x,z) and the evolution of atmospheric flow in time for each level and distance are presented by hövmoler diagram for velocity (x,t) or (z,t). Hövmoller diagram is a good method to visualize wave propagation along time evolution.

Fig.4 shows examples of a gravity wave evolution. The stable air flowing over a topographic barrier causes the atmospheric standing waves the so called mountain wave. By definition, the atmosphere becomes unstable when isentropes become vertical.

This wave being hydrostatic means that there is only one oscillation. Firstly, the wind is weak on the upstream side as expected in a blocking. The strongest winds are found over the lee slopes, but the storm does not extend far away from the mountains as which also depicted in Fig. 7 using periodic scheme either relaxation method. The nature of such waves is that the flow is fast where its movement is downward but slow where the flow ascends. Consequently there is fast flow on the lee slope of the mountain. In these graphs, horizontal wind denoted by red line refers to fast flow and green line describes slow flow. From that, it can be seen that a gravity wave appears after the first 2.5h (900) and more pronounce after 7.5h of simulations while vertical propagating waves can also be observed within the first wavelength of the mountain ridge barrier. Fig. 5-6 confirmed the evolution of velocity in each level as well as investigation through specific axis-point. It shows that in the lower level, the wind velocity is damped in front of mountain (upslope) and become faster in the back mountain (downslope). In many cases, these behavior could be observed by cap clouds indicate likely wave activity downstream. They often appear along mountain ridges as air is forced up the windward (upslope) side. But, it should be remembered that while cap clouds indicate likely wave activity absence, it does not mean that waves are absent too. It depends on the humidity or dry condition of the air flowing mountain. The vertically-wave propagating wave is also often most severe within the first wavelength downwind of the mountain barrier. These waves frequently become more amplified and tilt upwind with height which is very dangerous to and can cause aircraft to experience turbulence at high altitude.

In this simulation, the gravity wave does not propagate further creating lee wave trains (long distance propagation of gravity waves) due to breaking wave after 17.5 hour simulation at 8-9 km height. As naturally, vertically-propagating waves with sufficient amplitude may break in the lower troposphere, and theoretically can result turbulence within wave breaking region and nearby. If the propagating wave does not break, an aircraft would likely experience considerable wave action with a little turbulence.

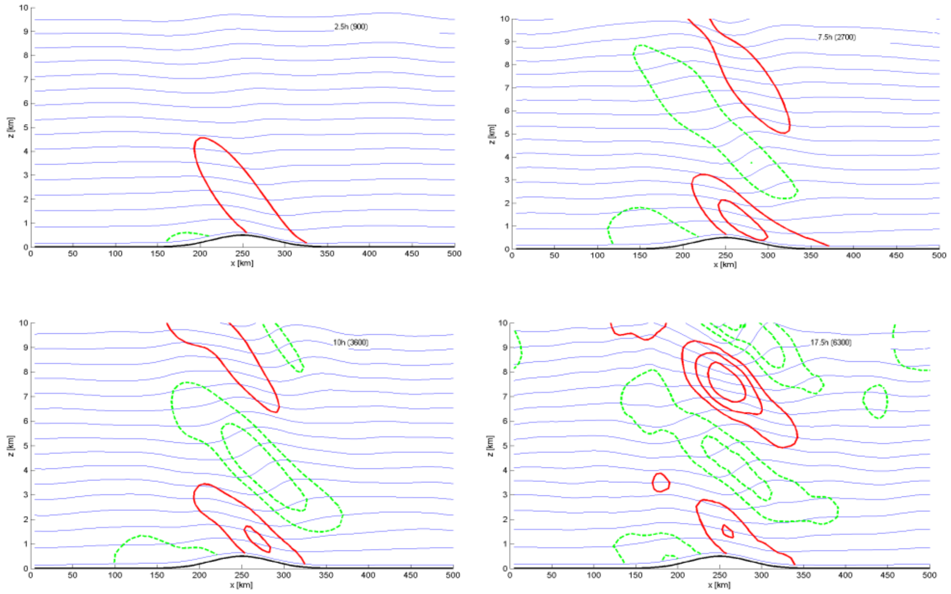

Figure 4. Isentropes obtained by numerical simulation with periodic lateral boundary at t = 2.5h(900), t=7.5h(2700), t=10h(3600) and t=17.5h(6300) and initial velocity 10ms^{-1}. Blue lines indicated potential temperature, and horizontal wind denoted by red line (stronger velocity) and green line (weaker velocity)

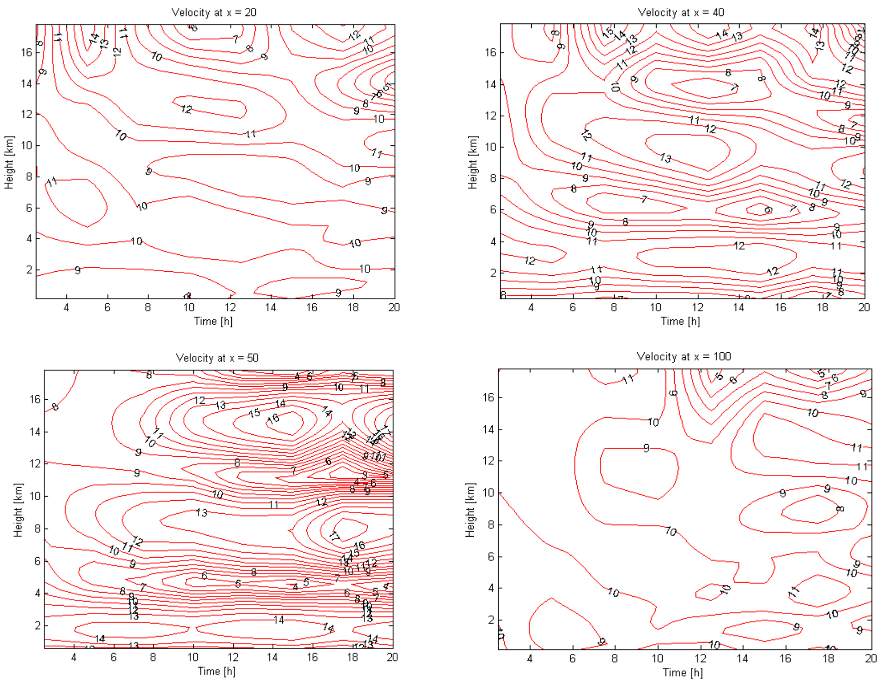

Figure 5. Hövmoller diagram describe ime-height cross section of velocity changes at specific point of horizontal distance.

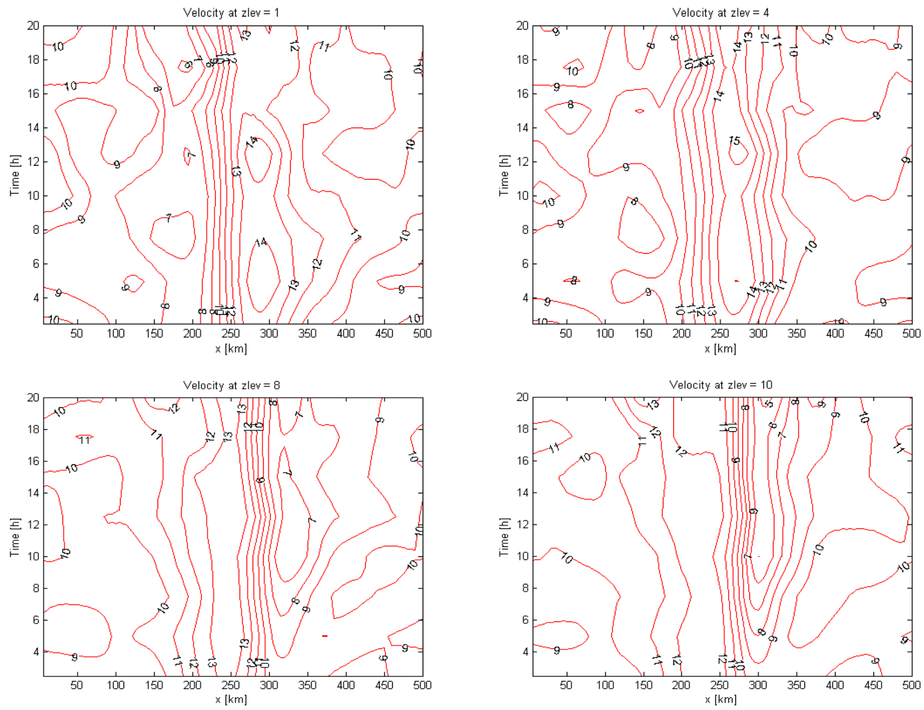

Figure 6. Hövmoller diagrams of velocity changes due to time evolution for each level of height along the horizontal distance.

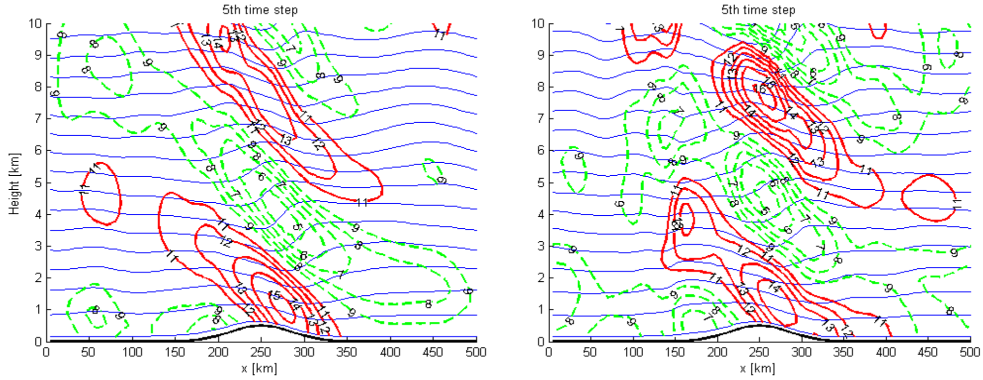

Figure 7. The differences result of numerical simulation using periodic (left) and relaxation (right) lateral boundary condition.

Additionally, in this simulation, the gravity wave as well as mountain wave can be observed well both using relaxation and periodic lateral boundary condition (Fig.7). Relaxation has been used here by absorbing wave energy along the boundary at the top of the isentropic profile. Simulation using relaxation mode therefore gives more realistic features.

Fig. 8 show that both mountain waves and downslope windstorms are sensitive to the size and the shape of the mountains (in this simulation is refers to the mountain height). The higher and bigger mountain may have stronger amplification and wave propagation as well as effect on the gravity wave generation and the lee velocity wave. For strong mountain waves and downslope windstorms to develop the wind should be directed roughly perpendicular to the mountain ridge. The wind speed should exceed about 20 ms^{-1} and there should be a stable layer not far from the mountain top level in the upstream temperature profile.

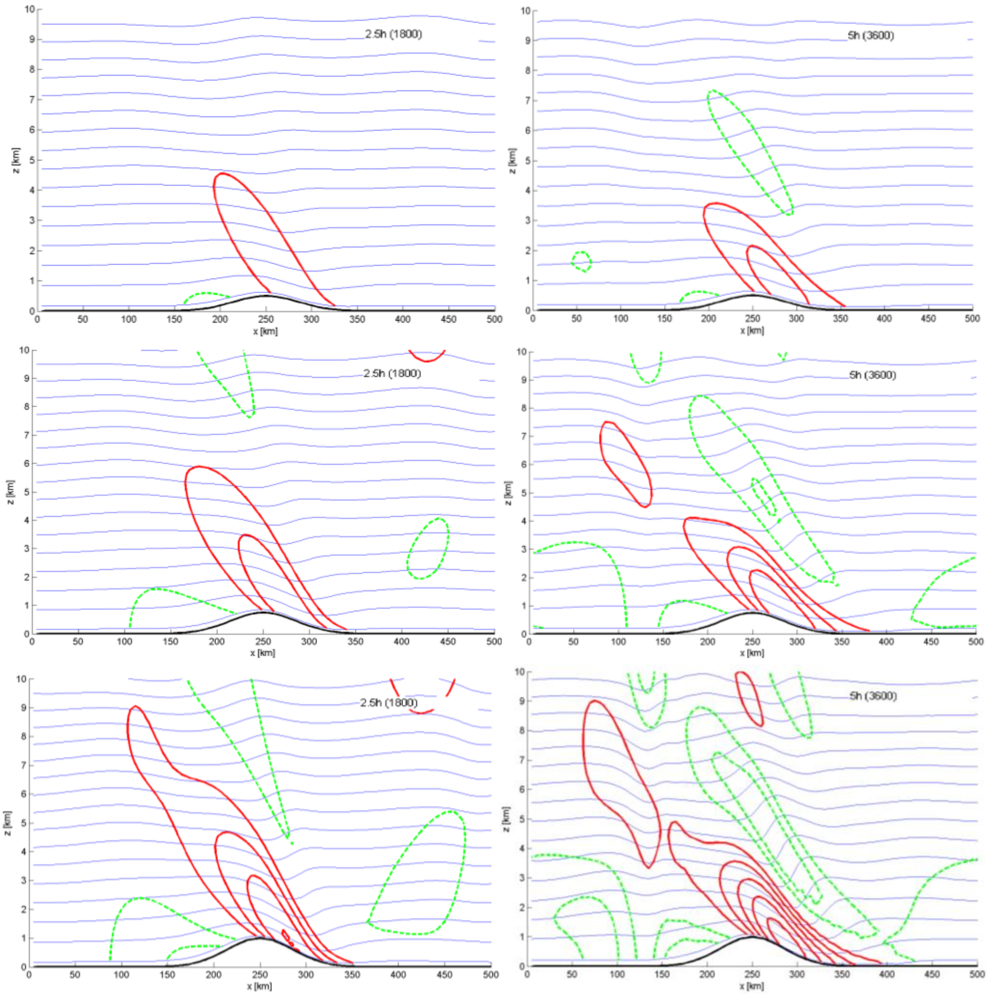

Figure 8. The simulation of sensitivity of gravity wave due to the mountain bell shape. Left panel show simulation at t = 2.5h(1800) and right panel show simulation at t=5h(3600) for mountain height h=500m (upper panel), h =750m (center) and h =1000m (bottom panel).

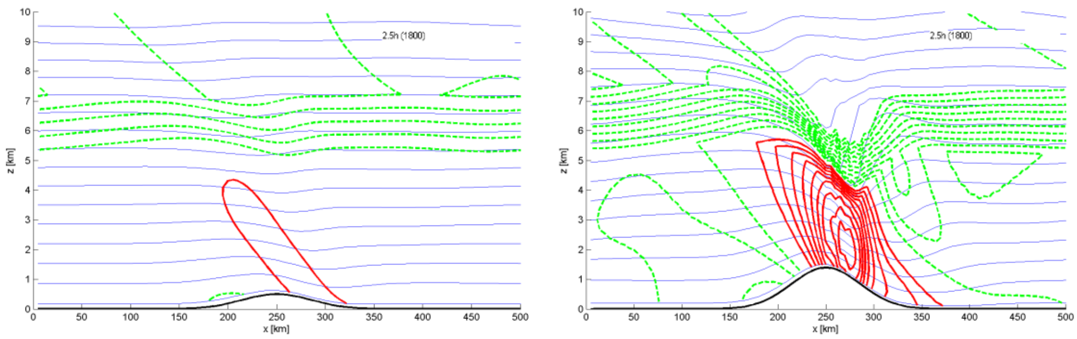

Figure 9. Windstorm obtained by numerical simulation with relaxation lateral boundary in the different mountain bell height. Simulation at t = 2.5h(1800) for mountain height h = 500m (left) and h = 1400m (right) with initial velocity 20 ms^{-1}.

The mean wind speed on the downslope (some time called as lee slope) can easily be many times the wind speed on the upstream side of the mountain. If the mountain waves are steep they may break in a similar manner as waves do on a beach (Fig 8). Strong downslope wind cases are usually associated with strong cross-barrier flow, waves breaking aloft, and an inversion near the barrier top. This may be double the wind speed at mountaintop level. Strong turbulence and wind shear at the surface are then associated with this high wind, causing significant danger to aircraft and damage at the surface too. In some cases, there is also strong turbulence in rotors that sometimes form in the wave field in the lee of the mountain below mountain top level. Gusts in downslope windstorms can easily be more than twice as strong as the 10 min average wind speed, making gustiness a characteristic of these storms and often abruptly end at the “jump region”, although more moderate turbulence can exist downstream.

Unfortunately, this work failed to simulate ‘jump’ phenomena that also very important in the mountain waves simulation.

5. CONCLUSION

From this early work, some conclusions are obtained due to the study of flow over the mountain ridges using isentropic model:

- A parcel of air within a stable air mass over a mountain will undergo wave motion.
- The resulting wave is gravity wave with up and downslope motions.
- Gravity waves can grow in amplitude until they ‘break’ into turbulence.
- If the magnitude of wind shear exceeds a critical value, turbulence will occur.

For the future work, it is important to investigate the wave characteristics by the Froude number adjustment in order to define vertically-propagating gravity wave. The Froude number expresses the ratio between kinetic energy (wind speed) and potential energy (stability times mountain height). Comparing the model simulation with observation such as using the satellite or wind radar analysis can also very important to develop an integration operational technique used to detect mountain wave signature.

6. REFERENCES

1. Durran, D. R., 1998. *Numerical Methods for wave equations in geophysical fluid dynamics. In Text in Applied Mathematics* (Vol. 32). Springer.

2. Holton, J. R., 2004. *Introduction to Dynamic Meteorology. Vol. 4.* Elsevier Academic Press.

3. Schär, C., 2009. *Numerical Modeling of Weather and Climate.* Institute for Atmospheric and Climate Science, ETH Zürich.

4. Schär, C., 2008. *Skript der Vorlesung "Numerische Methoden in der Umweltphysik".* http://www.iac.ethz.ch/people/schaer.